EPJ Web of Conferences **181**, 01029 (2018) https://doi.org/10.1051/epjconf/201818101029
EXA2017

Two Recent Developments in QCD Spectroscopy

Kamal K. Seth[1,⋆]

[1] *Northwestern University, Evanston IL 60208, USA*

Abstract. The presentation has two parts, the first, and main part, is devoted to the presentation of results from the first measurements of the production of Λ, Σ, Ξ and Ω hyperons at large timelike momentum transfers of 13.6, 14.2 and 17.4 GeV/c^2 made using e^+e^- annihilation data taken at the CESER election-positron collider at Cornell using the CLEOc detector. The measurements reveal interesting features of hyperon production systematics and timelike form factors, and provide evidence for diquark correlations in hyperon structure.
The second part of the presentation is devoted to measurements of photoproduction of J/ψ near threshold energies, $E_G = 8 - 12$ GeV, at the new photon physics facility, GlueX, at the Jefferson Laboratory. The first preliminary results are presented. These are expected to shed light on the gluon structure of protons, gluons which mediate the production of J/ψ in the reaction, $\gamma + p \to J/\psi + p, J/\psi \to e^+e^-$.

1 Introduction

The quark-gluon model of hadrons was introduced by Gell-Mann in 1956 to explain the structure of the quark-antiquark mesons and the three quark baryons which were the only hadrons known at that time. However, Gell-Mann suggested that other color-neutral hadrons containing larger number of quarks and antiquarks, as well as hybrids containing valence gluons, and glueballs containing only gluons should exist. These predictions launched numerous searches for these unconventional hadrons. Among the first of these was the search for six-quark "dibaryons". Many were proposed, and numerous claims and counter-claims were published. Unfortunately, none survived, and I myself claim responsibility for the demise of many of them [1]. Similarly, despite many dedicated searches during the last twenty years most claims for glueballs have not survived either [2].

These failures did not stop the searches by stubborn physicists that we are. But, so far no dibaryons or glueballs have been convincingly identified, and I will not talk about them.

However, a silver lining has recently emerged. Several convincing citings of the unconventional hadrons have been reported. An excellent summary of these exist in the 2011 compilation of QWG [3]. Subsequent updates have been presented in this conference by Belle and LHCb. With that said, I want to talk about only two developments in hadron spectroscopy in which I have been personally involved.

2 Hyperons

The major part of my talk is devoted to hyperons.

The universe is built of baryons. Before 1947 only two baryons, the proton and neutron, made of up and down quarks, were known. The 1947 discovery of the first strange particles, the kaon and the Lambda, and consequently, of the strange quark enriched the field of baryons immensely. By 1960, when the theoretically predicted Ω^- was discovered, all seven light baryons, containing strange quarks, Λ^0, Σ^0, Σ^+, Σ^-, Ξ^0, Ξ^- and Ω^-, known as hyperons, were known. However, even more than 50 years after their discovery very little more than the static properties of their ground states as listed in Table 1 are known [4].

Most of our extensive knowledge of nucleon structure comes from lepton scattering by nucleon and nuclear targets [5]. Unfortunately, hyperons are not available as targets, and this is responsible in large part for the lack of our understanding of the structure of hyperons.

In 1960 Cabibo and Gatto [6] pointed out that electron-positron colliders were being planned at various laboratories, and they offered opportunity of overcoming the lack of target disadvantage of hyperons; one could measure timelike form factors of hyperons in $e^+e^- \to B\bar{B}$ ($B \equiv$ hyperon) measurements. To put this opportunity in perspective, we note that four momentum transfers is defined as

$$Q(\text{4mom.})^2 = q(\text{3mom.})^2_{\text{space}} - (\text{energy})^2_{\text{time}} \qquad (1)$$

It can be positive and spacelike, as in scattering measurements, or negative and timelike, as in production measurements, as illustrated in Figure 1.

Form factors are analytic functions of momentum transfer $|Q|^2$, and $B\bar{B}$ pair production experiments can be analyzed in the same formalism as the scattering experiments, i.e., in terms of the Dirac form factor, $F_1(|Q|^2)$, and the Pauli form factor, $F_2(|Q|^2)$, or equivalently, in terms of

⋆e-mail: kseth@northwestern.edu

© The Authors, published by EDP Sciences. This is an open access article distributed under the terms of the Creative Commons Attribution License 4.0 (http://creativecommons.org/licenses/by/4.0/).

Table 1. The hyperon.

Hyperon	Quarks	Mass, M(MeV)	Mag.mom. (μ_N)	Main Decay
Proton, p	uud	938.272(<0.001)	2.793(<0.001)	stable
Λ^0	uds	1115.683(6)	-0.613(4)	$p\pi^-$(64%)
Σ^0	uds	1192.642(24)	1.61(8)	$\Lambda^0\gamma$(100%)
Σ^+	uus	1189.37(7)	2.458(10)	$p\pi^0$(52%)
Σ^-	dds	1197.449(30)	-1.160(25)	$n\pi^-$(99.8%)
Ξ^0	uss	1314.86(20)	-1.250(14)	$\Lambda^0\pi^0$(99.5%)
Ξ^-	dss	1321.71(7)	-0.6507(25)	$\Lambda^0\pi^-$(99.9%)
Ω^-	sss	1672.45(29)	-2.02(5)	Λ^0K^-(69%)

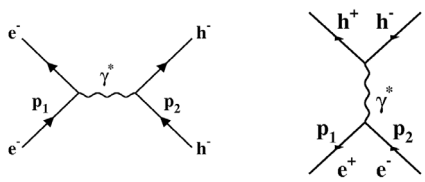

Figure 1. Spacelike and timelike four momentum transfers.

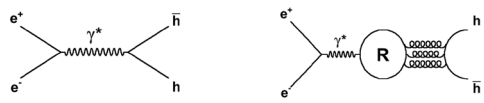

Figure 2. Electromagnetic decay and Hadronic decay via gluons.

Table 2. The estimation events from $\psi(3770)$ and $\psi(4170)$.

	$\Lambda\bar{\Lambda}$	$\Sigma^+\bar{\Sigma}^+$	$\Sigma^0\bar{\Sigma}^0$	$\Xi^-\bar{\Xi}^-$	$\Xi^0\bar{\Xi}^0$	$\Omega^-\bar{\Omega}^-$
$\psi(3770)$	3.0	1.4	1.2	1.2	0.6	0.3
$\psi(4170)$	2.0	1.0	0.9	0.9	0.4	0.2

the electric and magnetic form factors

$$G_E(|Q|^2) = F_1(|Q|^2) + (s/m^2)F_2(|Q|^2), \quad (2)$$

and

$$G_M(|Q|^2) = F_1(|Q|^2) + F_2(|Q|^2). \quad (3)$$

It took 30 years for the first successful measurement of $\Lambda^0\bar{\Lambda}^0$ hyperon production by the DM2 Collaboration at Orsay [7], and seventeen more years by the BaBar Collaboration at SLAC [8] to report measurements of $G_M(|Q|^2)$ of Λ^0, Σ^0, and the Λ^0 Σ^0 transition form factors. Because both these measurements were made near threshold energies $\sqrt{s} \approx 2.4$ GeV, and only a few events $4\Lambda^0\bar{\Lambda}^0$ by DM2, ≤ 22 by SLAC were observed, they were not suitable for QCD based analyses. No further progress in hyperon production studies was made until at CLEO in 2005 we made measurements of pair production of hyperons at the $\psi(2S)$ resonance, $\sqrt{s} = 3.69$ GeV, $|Q|^2 = 13.59$ GeV^2 [9].

We must remember, however, that unlike for spacelike form factors, G_E and G_M for timelike form factors do not relate to spatial distributions of charge and magnetic moment. Instead they relate to the helicity correlations between the particle antiparticle pair produced. $F_2(|Q|^2)$ denotes photon coupling to parallel spins and F_1 to antiparallel spins of the pair.

Hadronic decays at resonances proceed via gluons and have large yields. To measure electromagnetic form factors we require the decays to be electromagnetic, which have much smaller yields. To measure form factors we must measure e^+e^- annihilation at non-resonance energies, or at those resonances where it can be demonstrated that resonance yields are negligibly small, as $\psi(3770)$ and $\psi(4170)$ which mainly decay to $D\bar{D}$. Using the experimentally confirmed pQCD relation, schematically, illustrated below,

$$\frac{B(\psi(n')) \to \text{hadrons}}{B(\psi(n)) \to \text{hadrons}} = \frac{B(\psi(n')) \to \text{leptons}}{B(\psi(n)) \to \text{leptons}}, \quad (4)$$

we estimate the expected number of resonance events as in Table 2, i.e., at $\psi(3770)$ and $\psi(4170)$ the resonance contribution is indeed negligible for all hyperons, and the observed hyperon yield is entirely electromagnetic.

We have now made the world's first measurements of the pair production of Λ^0, Σ^0, Σ^+, Ξ^0, Ξ^- and Ω^- hyperons at large momentum transfers of 13.6, 14.2 and 17.4 GeV^2, and with good statistics. These measurements provide insight into the systematics of pair production of hyperons, the dependence of their cross section on their s-quark content, evidence for diquark correlations, and their timelike form factors. We use e^+e^- annihilation data taken at the CESR collider using the CLEO-c detector. The near-4pi acceptance CLEO-c detector, ilustrated in Figure 3, has cylindrical geometry and consists of a CsI electromagnetic calorimeter, drift chambers, and a RICH detector, all in a 1 Tesla solenoidal magnetic field. The data used in the measurements are listed in Table 3.

We identify the hyperons by detecting their major decay products, $\Lambda^0 \to p\pi^-$(64%), $\Sigma^+ \to p\pi^0$(52%), $\Sigma^0 \to \Lambda\gamma$(100%), $\Xi^- \to \Lambda\pi^-$(100%), $\Xi^0 \to \Lambda\pi^0$(100%), $\Omega^- \to \Lambda K^-$(68%). The $\psi(2S)$ resonance decay into hyperons has a prolific yield, and although it is not the subject

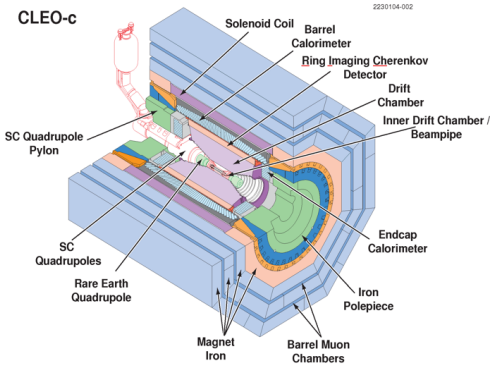

Figure 3. CLEO-c detector.

Table 3. The data used in the measurements.

	$\sqrt{s}$ (GeV)	$\lvert Q\rvert^2$ (GeV^2)	Luminosity (pb^{-1})
$\psi(2S)$	3.69	13.6	48
$\psi(3770)$	3.77	14.2	805
$\psi(4160)$	4.17	17.4	586

of my talk, Figures 4 and 5 illustrate the steps in hyperon identification very effectively.

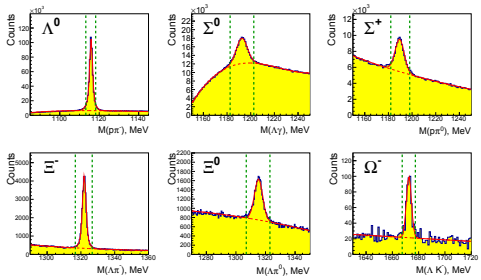

Figure 4. The six panels show the raw invariant mass distribution for $\psi(2S)$ data.

The six panels in Figure 6 show the invariant mass distribution of $B\bar{B}$ pair production events of Figures 4. The six panels in Figure 7 show event distribution for $\psi(3770)$ data for electromagnetic production of hyperons with backgrounds due to inclusive production of single hyperons.

In Table 4 we present the summary of pair production cross sections. We note that the cross sections for electromagnetic production at $\psi(3770)$ are smaller by factors $\geq$ 200 than for the resonance production at $\psi(2S)$. The VDM theoretical predictions of Körner and Kuroda [10] for $\psi(3770)$ are smaller by orders of magnitude than our measured values. The top panel in Figure 8 illustrates the variation of cross sections for hyperon pair production at

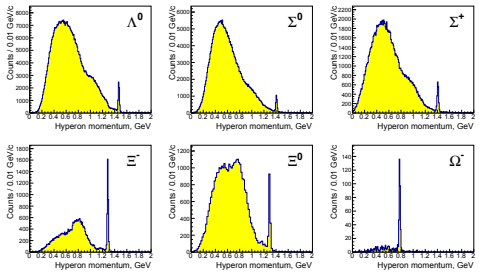

Figure 5. The six panels show the momentum distribution for $\psi(2S)$ data. The large yields on left correspond to inclusive production and the sharp peaks on right to exclusive $B\bar{B}$ pair production.

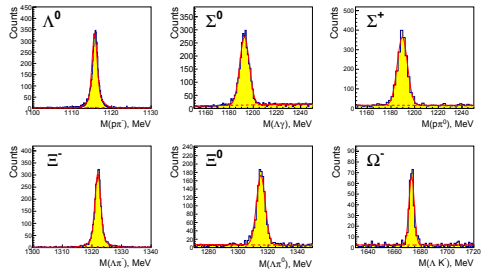

Figure 6. $\psi(2S)$ pair production: the numbers of observed events are $N(\Lambda, \Sigma^0, \Sigma^+) = 6531, 2645, 1874$, $N(\Xi^-, \Xi^0, \Omega) = 3580, 1242, 326$.

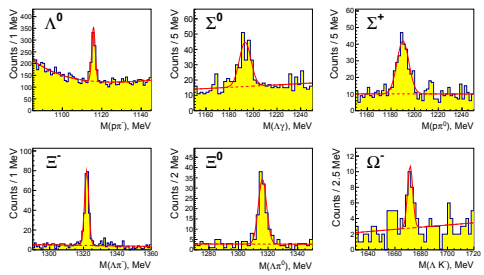

Figure 7. $\psi(3770)$ pair production: the numbers of observed events are $N(\Lambda, \Sigma^0, \Sigma^+) = 498, 142, 200$, $N(\Xi^-, \Xi^0, \Omega) = 240, 111, 20$. Notice an order or more decrease than the resonance yield at $\psi(2S)$.

$\psi(3770)$. It shows that $\sigma(\Sigma^0)$ is much smaller than the general trend of the data for $J = 1/2$ hyperons, and nearly factor 2.3 ± 0.4 smaller than $\sigma(\Lambda^0)$ which has the same uds quark construct. The bottom panel in Figure 8 illustrates an unexpected feature, the ratio $\sigma(3770)/\sigma(4170)$ does not vary as $1/s^5$ as pQCD predicts, but shows steps with increasing number of s-quarks in the hyperonss. More about this very important observation later.

Table 4. Summary of pair production cross sections (picobarns), and $G_M(3770)$.

	p	Λ^0	Σ^0	Σ^+	Ξ^-	Ξ^0	Ω^-	$\Lambda^0\Sigma^0$
$\psi(2S)$	196(12)	244.7(106)	145.6(77)	151.4(74)	199.9(100)	131.6(82)	33.7(28)	8.1(16)
$\psi(3770)$	0.46(4)	1.13(10)	0.46(8)	0.97(10)	0.78(7)	0.68(9)	0.11(3)	0.43(9)
VDM Theory $\psi(3770)$ [10]	0.069	0.010	–	0.081	0.064	0.014	0.006	0.042
$G_M(3770)$	0.88(4)	1.40(6)	0.91(7)	1.31(7)	1.20(5)	1.12(6)	0.53(8)	0.77(8)

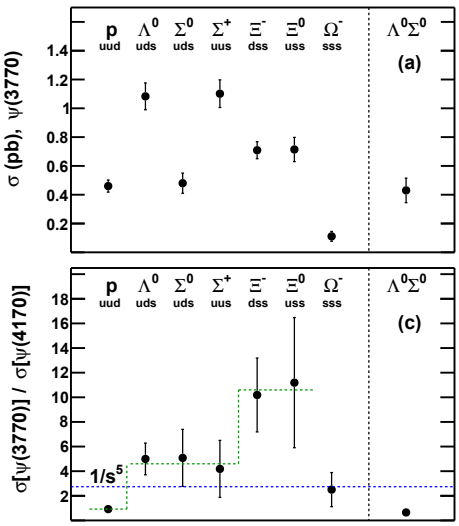

Figure 8. The cross sections from $\psi(3770)$ and $\psi(4170)$ data. Note steps at number of strange quark, $S = 0, 1, 2$.

As for nucleons, the timelike form factors are related to cross sections in terms of form factors G_E and G_M, which now refer to correlations between the helicities of the baryon and antibaryon

$$d\sigma/d\Omega = \frac{\alpha^2\beta_B}{4s}[|G_M^B(s)|^2(1+\cos^2\theta) + (4m_B^2/s)|G_E^B(s)|^2\sin^2\theta], \quad (5)$$

$$\sigma_{B\bar{B}} = \frac{4\pi\alpha^2\beta_B}{3s}\left(|G_M^B(s)|^2 + (2m_B^2/s)|G_E^B(s)|^2\right). \quad (6)$$

Because of small yield of hyperons from electromagnetic decays, it is generally not possible to determine G_E and G_M, or G_E/G_M separately, and most experimental data are analyzed by assuming $G_E/G_M = 0$ or 1.

BaBar has recently analyzed the angular distributions for their ISR based production of $\Lambda\bar{\Lambda}$ pairs in two vs bins. They obtained $|G_E/G_M| = 1.73^{+0.99}_{-0.57}$ for the $\sqrt{s} = 2.23 - 2.40$ GeV/c^2 bin with 115 events, and $|G_E/G_M| = 0.71^{+0.66}_{-0.71}$ for the $\sqrt{s} = 2.40 - 2.80$ GeV/c^2 bin with 61 events. They considered both of them as consistent with $G_E/G_M = 1$, and analyzed their data with that assumption.

We note that because of their large errors BaBar's results are equally consistent with $G_E/G_M = 0$. We have analyzed our data for Λ^0, Ξ^0, Ξ^- production, and obtained $G_E/G_M = 0$ in all three cases, with 90% confidence limits: $\Lambda^0 < 0.17, \Xi^0 < 0.32, \Xi^- < 0.29$. Unexpected as this result is, it is consistent with the recent Jlab observation, $G_E = 0$ at $|Q|^2 \approx 8$ GeV^2 for spacelike form factor of proton. We have analyzed our data for $|Q|^2$=14.2 and 17.4 GeV^2 assuming $G_E = 0$. The results for $\psi(3770)$ are presented in Table 4. Unfortunately, unlike for the proton there are no measurements of spacelike form factors hyperons to compare with.

We note that these are the first measurements ever of these timelike form factors of hyperons at such large momentum transfer. There are no VDM or QCD based predictions for them. We note that G_M for all $J = 1/2$ hyperons are the same within a factor ~ 1.5. We note that $G_M(\Lambda)/G_M(\Sigma^0) = 1.5 \pm 0.1$.

Figure 9 illustrates variation of $G_M(3770)$, and the steps in the ratio $G_M(3770)/G_M(4170)$ with increasing number of strange quarks. Figure 10 shows the rapid decrease of inclusive hyperon production from Λ^0, to $\Sigma^{0,+}$, to $\Xi^{0,+}$, and finally to $J = 3/2$ Ω^-.

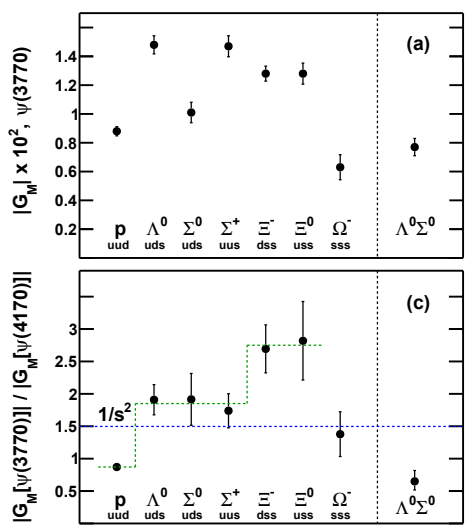

Figure 9. The G_M results from $\psi(3770)$ and $\psi(4170)$ data. Note steps at $S = 0, 1, 2$.

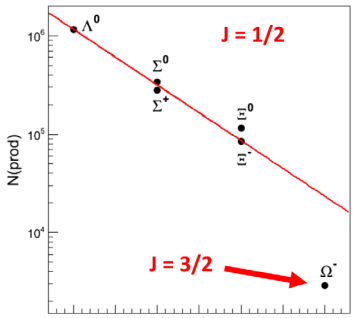

Figure 10. An interesting trend for inclusive events produced with $\mathcal{L}$=48 pb^{-1} at $\psi(2S)$.

3 Diquark in hyperons

Our most important result concerns the evidence for diquark correlations in hyperon pair production. The importance of certain configurations of flavor, spin, and isospin of two quarks in the structure of hadrons has been recognized for a long time [12]. One dramatic example of the role of diquarks was provided by the Fermilab observation that the timelike form factor of the proton was twice as large as the spacelike form factor at the same large momentum transfer $|Q|^2$ [13], and its successful explanation by Kroll et al. [14] in terms of the diquark-quark structure of the proton.

Recently Wilczek and colleagues [15] have emphasized the role of diquarks in QCD in terms of isoscalar "good", and isovector "bad" diquarks. They predicted that the "good" diquark in Λ^0 with isospin 0 compared to the "bad" diquark in Σ^0 with isospin 1, would lead to enhancement of Λ^0 over Σ^0 in production experiments. They cited the observation of $\Lambda^0/\Sigma^0 = 3.5 \pm 1.7$ in the LEP experiment in support of this prediction.

Our measurements provide strong independent support for the role of diquarks in Λ^0/Σ^0 hyperon production. We observe $\sigma(\Lambda^0)/\sigma(\Lambda^0) = 2.46 \pm 0.46$ at $|Q|^2 = 14.2$ GeV^2 (in exclusive pair production), $\sigma(\Lambda^0)/\sigma(\Lambda^0) = 2.56 \pm 1.40$ at $|Q|^2 = 17.4$ GeV^2 (in exclusive pair production), $\sigma(\Lambda^0)/\sigma(\Lambda^0) = 4.1 \pm 0.6$ at $|Q|^2 = 13.6$ GeV^2 (in inclusive pair production). Our data provide the opportunity to consider diquark pairs other than the up/down diquarks, and we expect that they will lead to a deeper understanding of diquark correlations. Lattice calculations are also expected to address diquark correlations soon [16].

4 Threshold photoproduction of J/ψ

The second part of my talk is not about a new subject like hyperons, but an old subject: Threshold photoproduction of J/ψ. The discovery of J/ψ in $e^+e^- \to \gamma^* \to J/\psi$ launched the modern era in QCD spectroscopy. Despite the fact that all particle physics experiments cut their teeth on the detection of J/ψ, it remains true that J/ψ production mechanisms are not well understood. There are theoretical models to be sure, color singlet model, color evaporation model, factorization models, etc., but serious problems in quantitative understanding of J/ψ production remain. Of particular interest is understanding photoprouction of J/ψ at energies near threshold, E_γ ~8.5 GeV, because at small momentum transfers coherent electro production of vector mesons like ϕ, J/ψ, etc. provides valuable insight into the gluon structure function of the target [17].

Gluon distribution functions at small x have been of interest in relation to studies of deconfinement in QGP, the phenomena of color transparency and others, and good precision data on J/ψ photo production near threshold energies has long been needed to distinguish between models of gluon structure functions.

Brodsky et al. have made a more detailed study of J/ψ photoproduction and predicted that near threshold the J/ψ production cross sections have very different dependence on the momentum of photons depending on whether two or three gluons carry the targets momentum to the charm quarks [18] (Figure 11). The existing data consists of just two small statistics measurements by Cornell [19] and SLAC [20], and they are too sparse to distinguish between the two models (Figure 12).

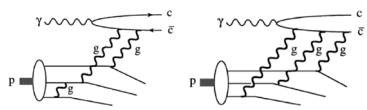

Figure 11. J/ψ production in two/three gluons processes.

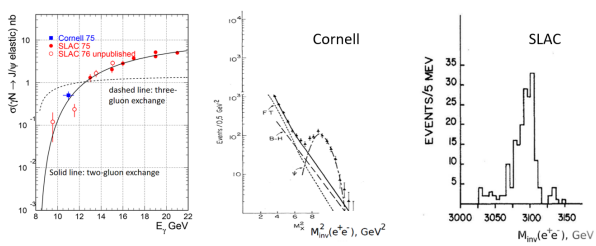

Figure 12. Left: Theoretical predictions for 2/3 gluon production of J/ψ. Right: Existing measurements by Cornell [19] and SLAC [20].

At the Jefferson lab we now have polarized and unpolarized electron beams of energies up to 12 GeV available, and a facility called GlueX has been constructed, dedicated to photo production experiments (Figure 13). This has made it possible to fill the gap in threshold measurements of J/ψ photo production. We have made the first such measurements of $\gamma + p \to p + J/\psi, J/\psi \to e^+e^-$, and I want to present the first results of these measurements which we believe shed valuable light on the gluon content of protons and their role on J/ψ photo produc-

tion. Figure 13 shows the photon beam production and the schematic of the GlueX detector.

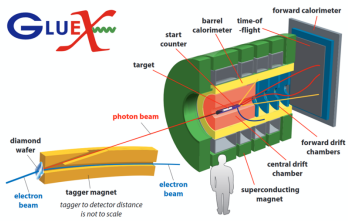

Figure 13. The GlueX detector.

We have made the first successful measurements of $\gamma + p \rightarrow p + J/\psi, J/\psi \rightarrow e^+e^-$ with tagged photons of energies between 8 and 12 GeV at the GlueX facility at Jlab. I will not bore you with the details of event selection for these, but here are a few details: (1) At least 3 charged tracks are required in the event. (2) The yield of the e^+e^- decays are overwhelmed by more than three orders of magnitude larger production of the Bethe-Heitler production of $\pi^+\pi^-$ pairs. To reject the $\pi^+\pi^-$ BH background we use the quantity E/p, with E from EM calorimeter and p from drift chambers. E/p$\sim$ 1 for electrons, and is much smaller for pions. We require E/p$>$ 0.8 for the selected events, which selects e^+e^- events very effectively, and provides very good rejection of the pion background.

Brodsky et al [18] pointed out that the negative charge conjugation J/ψ can be populated in photoproduction mainly by transition of two gluons from the proton target $\gamma + 2g$. If convincing evidence is found for three gluon transition $\gamma + 3g$, the gluons have to carry orbital angular momentum in addition to spin. This possibility is of great fundamental importance to QCD in many contexts, e.g., in context of the famous problem of proton spin, and it has been long studied by means of deep inelastic scattering. If our measurements of J/ψ photoproduction in the threshold region provide evidence for 3-gluon transition, we will have made a major contribution to QCD itself.

We have made two measurements of J/ψ photoproduction in the threshold region, in Feb. 2016 ($E_\gamma = 8 - 12$ GeV), and in Feb. 2017 ($E_\gamma = 8 - 11.5$ GeV), whose invariant mass spectra are shown in the Figure 14. Population of the vector resonances J/ψ and ϕ are clearly observed. The detailed plot of our observed J/ψ spectrum is shown in Figures along with the results of the earlier referred measurements of SLAC and Cornell, for comparison. I have to disappoint you by telling you that we are not yet able to quote production cross sections or their all important energy dependence. We expect to be able to do so in about three months. Keep tuned.

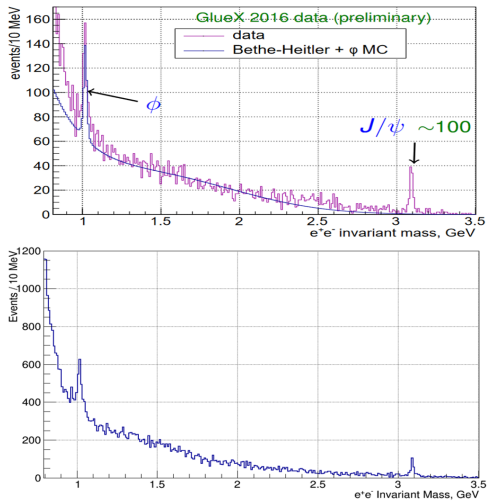

Figure 14. The J/ψ from GlueX in 2016 and 2017.

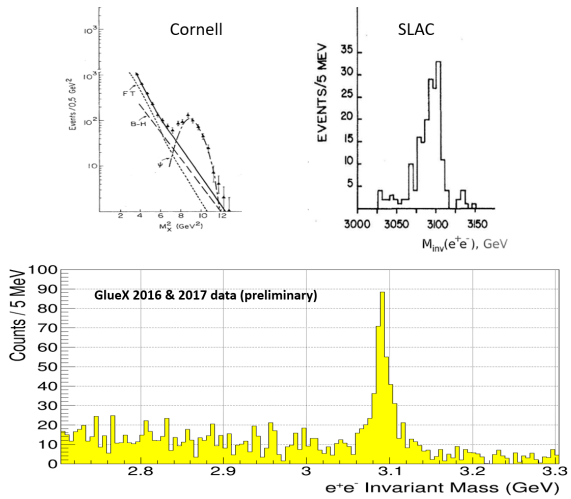

Figure 15. The preliminary result from GlueX.

References

[1] Kamal K. Seth, Proc. Few Body XII Conference, TRIUMF (1989) TRI 89-2, p. C35

[2] S. Dobbs et al., Phys. Rev. D **91**, 052006 (2015)

[3] N. Brambilla et al., Eur. Phys. J. C **71**, 1534 (2011)

[4] C. Patrignani et al. Particle Data Group, Chinese Phys. C, 40 (2016)

[5] For reviews of spacelike data, see: J. Arrington et al., J. Phys G **34**, 523 (2007); C. F. Perdristat et al., Prog. Particle and Nucl. Phys. **59**, 694 (2007)

[6] N. Cabibbo and R. Gatto, Phys. Rev. Lett. **313**, 4 (1960); Phys. Rev. **124**, 1577 (1961)

[7] D. Bisello et al. [DM2 Collaboration], Z. Phys. C **48**, 23 (1990)

[8] B. Aubert et al. [BaBar Collaboration], Phys. Rev. D **76**, 092006 (2007)

[9] T. K. Pedlar et al. [CLEO Collaboration], Phys. Rev. D **72**, 051108 (2005)

[10] J. G. Körner and M. Kuroda, Phys. Rev. D **16**, 2165 (1977)

[11] A. Z. Dubnickova et al, Czech. J. Phys. **43**, 1177 (1993)

[12] M. Anselmino et al., Rev. Mod. Phys. **65**, 1199 (1993)

[13] T. A. Armstrong et al. PRL **70**, 1212 (1993); M. Ambrogiani et al., Phys. Rev. D **60**, 032002 (1999)

[14] P. Kroll et al., Phys. Lett. B **316**, 546 (1993)

[15] R. Jaffe and F. Wilczek, Phys. Rev. Lett. **91**, 232003 (2003); F. Wilczek, Diquarks as inspiration and as objects, in: M. Shifman, et al. (Eds.), From Fields to Strings, vol. 1. World Scientific, Singapore, 2005, pp. 77-93, arXiv: hep-ph/0409168; A. Selem et al., arXiv: hep-ph/0602128;

[16] For lattice calculations of hyperons, see R. Babich et al., Phys. Rev. D **76**, 074021 (2007); J. Green et al., Proc. Sci. (LATTICE 2010), 140 [arXiv:1012.2353]

[17] Brodsky, et al. PRD **50**, 3134 (1994); D. Kharzeev, et al., Nucl. Phys. **A661**, 568 (1999); L. Frounkfuzt and M. Strikman, PRD **66**, 031502 (R) (2002)

[18] S. J. Brodsky et al., Phys. Lett. B **498**, 23 (2001)

[19] Gittleman et al., PRL **35**, 1616 (1975)

[20] Camerini et. al., PRL **35**, 483 (1975)